Cancer Research

Lactate Influx through the Endothelial Cell Monocarboxylate Transporter MCT1 Supports an NF-κB/IL-8 Pathway that Drives Tumor Angiogenesis

Frédérique Végran[1], Romain Boidot[1], Carine Michiels[2], Pierre Sonveaux[1], and Olivier Feron[1]

Abstract

Lactate generated from pyruvate fuels production of intracellular NAD^+ as an end result of the glycolytic process in tumors. Elevated lactate concentration represents a good indicator of the metabolic adaptation of tumors and is actually correlated to clinical outcome in a variety of human cancers. In this study, we investigated whether lactate could directly modulate the endothelial phenotype and thereby tumor vascular morphogenesis and perfusion. We found that lactate could enter endothelial cells through the monocarboxylate transporter MCT-1, trigger the phosphorylation/degradation of IκBα, and then stimulate an autocrine NF-κB/IL-8 (CXCL8) pathway driving cell migration and tube formation. These effects were prevented by 2-oxoglutarate and reactive oxygen species (ROS) inhibitors, pointing to a role for prolyl-hydroxylase and ROS in the integration of lactate signaling in endothelial cells. PHD2 silencing in endothelial cells recapitulated the proangiogenic effects of lactate, whereas a blocking IL-8 antibody or IL-8–targeting siRNA prevented them. Finally, we documented in mouse xenograft models of human colorectal and breast cancer that lactate release from tumor cells through the MCT4 (and not MCT1) transporter is sufficient to stimulate IL-8–dependent angiogenesis and tumor growth. In conclusion, our findings establish a signaling role for lactate in endothelial cells and they identify the lactate/NF-κB/IL-8 pathway as an important link between tumor metabolism and angiogenesis. *Cancer Res; 71(7); 2550–60.* ©*2011 AACR.*

Introduction

Tumor cells fuel their metabolism with a variety of nutrients including glucose, glutamine, and lactate to meet the bioenergetic and biosynthetic demands of proliferation (1, 2). Glycolysis coupling to the tricarboxylic acid (TCA) cycle and oxidative phosphorylations, is actually far to be the unique source of energy. Hypoxia and oncogenic mutations drive glucose to pyruvate transformation and then pyruvate to lactate conversion ensuring the regeneration of the NAD^+ pool necessary to support a high glycolytic flux to fulfil the demand for ATP and precursors (a phenomenon called the Warburg effect when occurring in the presence of sufficient oxygen). Also independently of a coupling to the oxidative phosphorylations, the TCA cycle may act as a biosynthetic hub fed by 2-oxoglutarate arising from glutaminolysis (3). Moreover, glycolysis and glutaminolysis share the capacity to generate NADPH, from the pentose phosphate pathway and indirectly through the malate conversion into pyruvate, respectively. The latter pathway may also contribute to an additional source of NAD^+ through the conversion of pyruvate into lactate (1). In tumors, both glycolysis and glutaminolysis therefore lead to the production of lactate. Interestingly, as previously documented in muscle fibres and brain (4, 5), lactate may in turn be taken up by oxygenated (tumor) cells to feed oxidative metabolism (1). We recently documented that this can contribute to reduce consumption of glucose (and probably glutamine) by tumor cells at the vicinity of blood vessels and thereby to increase the availability of these substrates for hypoxic tumor cells (6). One may thus propose that tumor lactate levels and fluxes reflect the extent of the adaptation of tumor cells to survive and proliferate.

A role of lactate in malignancy is supported by studies documenting a correlation between tumor lactate levels and clinical outcome in a variety of human cancers (7–13). In particular, high lactate levels were found to be associated with a high incidence of distant metastases already in early stages of the disease and inversely, longer survival was associated with low lactate concentrations in tumors. Among the possible mechanisms supporting these clinical data, lactate is proposed to stimulate angiogenesis (14–17) through an activation of the VEGF/VEGFR2 signaling pathway (18–20); a parallel lactate-induced TGFβ-1-mediated pathway was also

Authors' Affiliations: [1]Université catholique de Louvain, Pole of Pharmacology & Therapeutics (UCL-FATH), Angiogenesis & Cancer Research Laboratory, Institute of Experimental and Clinical Research (IREC), Brussels, Belgium; and [2]University of Namur (FUNDP), Unit of Research in Cellular Biology (URBC), Namur, Belgium

Note: Supplementary data for this article are available at Cancer Research Online (http://cancerres.aacrjournals.org/).

Corresponding Author: Olivier Feron, Pole of Pharmacology and Therapeutics, UCL-FATH5349, 52 avenue E. Mounier, B-1200 Brussels, Belgium. Phone: 32-2-764-5264; Fax: 32-2-764 5269; E-mail: olivier.feron@uclouvain.be

doi: 10.1158/0008-5472.CAN-10-2828

proposed to prevent maturation of neoformed tubes (21). Because of the known HIF-mediated regulation of VEGF (22) and the capacity of glycolytic carboxylate intermediates including pyruvate and lactate to stimulate hypoxia-inducible factor (HIF) expression (23, 24), the effects of lactate on VEGF (and angiogenesis in general) are thought to be HIF-1α–dependent (16).

As major metabolic pathways in tumors end up with lactate secretion and because this may occur under both hypoxic and nonhypoxic conditions (Warburg effect), we reasoned that lactate could act as a signaling molecule in endothelial cells through not only HIF-dependent but also -independent pathways. Furthermore, although hypoxia-independent expression of HIF-1 is possible in tumor cells in response to oncogenic or loss-of-function mutations pathways (22, 25), this is not occurring in genetically stable endothelial cells. Also, the paradigmatic HIF1-dependent angiogenic growth factor VEGF is produced to much larger extent by tumor cells or tumor-associated macrophages than by endothelial cells (10- to 50-fold more at the protein level, unpublished data). Thus, to examine a possible autocrine pathway in endothelial cells triggered by lactate arising from tumor cells, we first used a low density array strategy to identify possible actors. This initial exploration led us to document that lactate could promote a PHD2- and ROS-dependent NF-κB activation in endothelial cells. We further identified the monocarboxylate transporter MCT1 as the main gate for lactate entry in endothelial cells and the consecutive production of IL-8/CXCL8 as an autocrine signal mediating the effects of lactate on angiogenesis and tumor perfusion.

Materials and Methods

Cell culture and treatments

Human colorectal adenocarcinoma WiDr cells and MDA-MB231 breast cancer cells were obtained from the American Type Culture Collection Cell lines where they are regularly authenticated based on viability, recovery, growth, morphology, and isoenzymology. WiDr cells and MDA-MB231 cells were acquired in 2009 and 2010, respectively, stored according to the supplier's instructions, and used within 6 months after resuscitation of frozen aliquots. Human umbilical vein endothelial cells (HUVEC) were used within 6 months of purchase from Sigma, acting as a distributor for ECACC (European Collection for Cell Cultures). HUVECs were routinely cultured in endothelial cell basal medium (Sigma) and used between passages 2 and 5. In some experiments, cells were treated with an anti-IL-8–neutralizing antibody (R&D systems), evodiamine (Calbiochem), or *N*-acetyl-*L*-cysteine (Sigma) in glucose- or lactate-containing medium.

Mouse models

For *in vivo* experiments, NMRI nude mice (Elevage Janvier) were injected subcutaneously with 400 μL Matrigel containing one of the following combinations: (i) 5×10^5 tumor cells (WiDr or MDA-MB231) mixed with 5×10^4 HUVEC cells, with or without IL-8–blocking antibody; (ii) 5×10^5 WiDr shMCT1 or 5×10^5 WiDr shMCT4 cells mixed with 5×10^4 HUVEC cells; (ii) 5×10^5 MDA-MB231 or 5×10^5 MDA-MB231 shMCT4 cells mixed with 5×10^4 HUVEC cells. Tumor sizes were tracked with an electronic calliper, and tumors were collected after the animal sacrifice 14 days after injection. In some experiments, local tumor blood flow was measured with a Laser Doppler imager (Moor Instruments) on anesthetized mice as previously described (26).

Real-time PCR and silencing experiments

PCR amplification was performed in an IQ5 Thermocycler (Bio-Rad); primers sequences are described in Supplementary Data. For gene expression profiling, Taqman Angiogenesis Gene signature Arrays (Applied Biosystems Inc.) were used according to the manufacturer's instructions. For siRNA silencing experiments, HUVEC cells were transfected (LipofectAMINE 2000; Invitrogen) with specific siRNA (Qiagen), whereas for shRNA silencing experiments, BLOCK-iT H1 RNAi Entry Vector Kit (Invitrogen) was used. Sequences are described in Supplementary Data.

IL-8 ELISA, NF-κB luciferase reporter, and DNA binding assays

The extent of IL-8 production by HUVEC and tumor xenografts was determined in an ELISA assay (QuantiGlo Chemiluminescent Immunoassay; R&D systems). The luciferase reporter pNF-κB-Luc plasmid (Stratagene) was transfected 24 hours before cell treatments; a GFP-expressing vector was cotransfected to adjust for variations in transfection efficiencies. DNA binding of NF-κB subunit p65 was determined using a TransAM ELISA kit (Active Motif).

Reactive oxygen species measurements and lactate measurements

Intracellular reactive oxygen species (ROS) were assessed using oxidation-sensitive probe 2′,7′-dichlorofluorescein diacetate (DCFH-DA; Sigma). Lactate concentration was determined via the lactate dehydrogenase (LDH)-catalyzed oxidation of lactate into pyruvate in the presence of NAD^+ (6).

Endothelial cell migration and tube formation assays

HUVEC cell mobility and migration were evaluated in a modified Boyden chamber assay using transwell filters inserts with 8-μm pore size (Greiner Bio-one). The formation of capillary-like endothelial tubes was determined in an *in vitro* assay by plating endothelial cells on growth factor-reduced Matrigel (BD Pharmingen), as previously reported (27, 28).

Immunostaining and immunoblotting

Tumors were cryosliced and sections were probed with a rat monoclonal antibody against CD31 (BD PharMingen) or rabbit polyclonal antibodies against MCT1 (Millipore) and MCT4 (Polypetide) followed by a secondary antibody coupled to an Alexa Fluor-568 as previously described (6, 29). For immunoblotting, cells extracts were separated on SDS-PAGE and transferred onto PVDF membranes before incubation with the MCT1 (Millipore), IκBα (Millipore) and phospho-serine 32 and36 IκBα (Cell Signaling) antibodies; gel loading was normalized with a beta-actin antibody (Sigma).

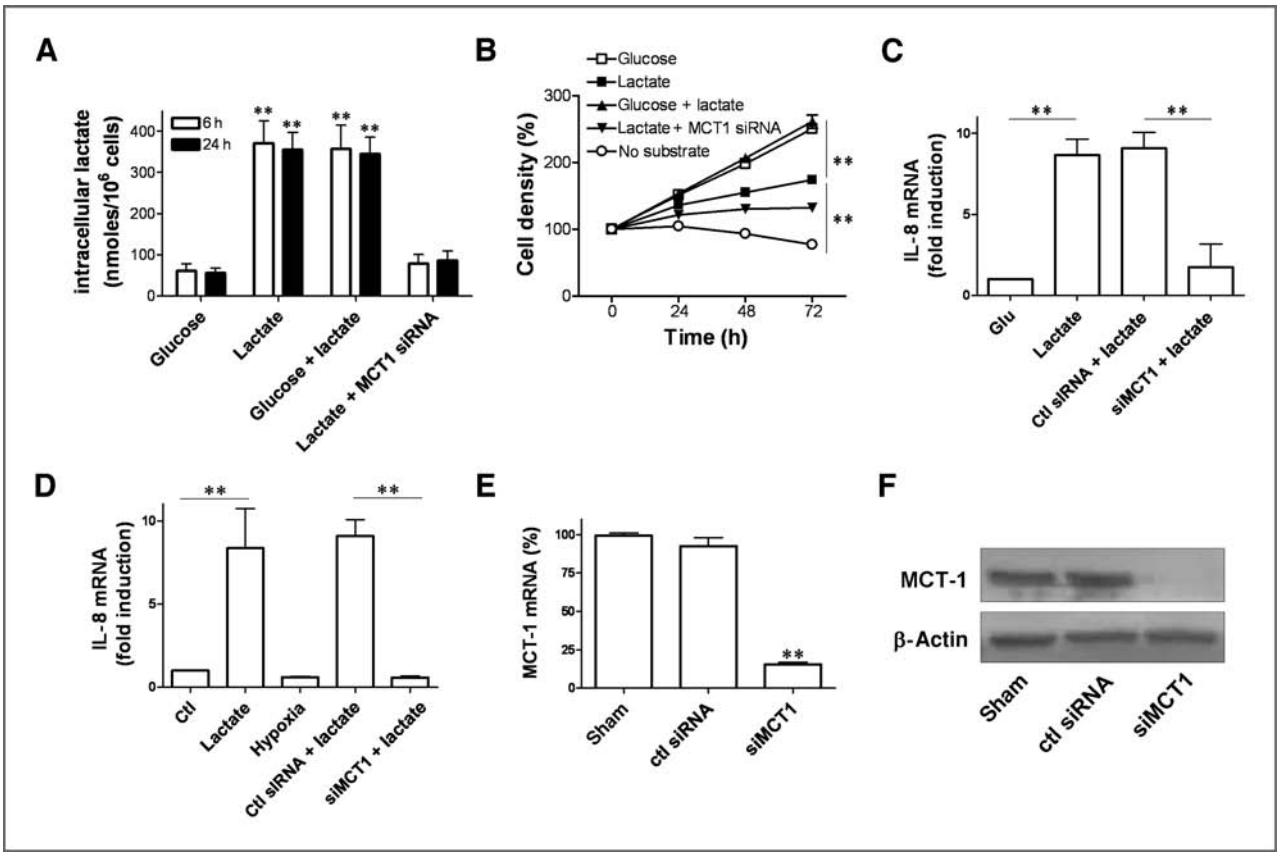

Figure 1. MCT1-dependent lactate uptake in endothelial cells stimulates IL-8 expression. Endothelial cells were exposed to medium containing glucose, lactate (10 mmol/L), glucose + lactate, or none of the aforementioned; in some experiments, cells were first transfected with a MCT1-targeting siRNA (or a control siRNA) or incubated under 1% O_2 for the same period of time. Graphs represent these different conditions: (A) the intracellular lactate concentrations determined after 6 and 24 hours of treatment, (B) the extent of cell proliferation after 24, 48, and 72 hours, (C) IL-8 mRNA levels as determined by qPCR, and (D) IL-8 protein expression as determined by ELISA. **, $P < 0.01$, $n = 3$ to 4. MCT1 silencing with dedicated siRNA (vs. sham conditions and control siRNA) was confirmed (72 hours posttransfection) by qPCR (E) and by immunoblotting as shown in a representative Western blot (F); β-actin signal is used as a gel loading control. **, $P < 0.01$, $n = 3$ to 4.

Statistics

Results are expressed as mean ± SEM. Student's *t* test, 1-way ANOVA (Tukey's *post-hoc* test), were used where indicated. *, $P < 0.05$ or **, $P < 0.01$ was considered statistically significant in the different experiments.

Results

MCT1-driven lactate uptake in endothelial cells promotes IL-8 expression

We first determined the capacity of lactate to be taken up by endothelial cells and to influence cell proliferation. We found that independent of the presence or the absence of glucose, the addition of 10 mmol/L lactate in the culture medium led to a net increase in intracellular lactate concentration reaching 6-fold the level of lactate observed in the presence of glucose-containing (lactate-free) medium (Fig. 1A). This elevated level of cytosolic lactate was reached after 1 hour of exposure to extracellular lactate and then maintained itself around the newly setup basal value, independently of the lactate concentration in the medium as long as established between 1 and 25 mmol/L (not shown). Although no sign of cell death (i.e., cell detachment) could be observed, the presence of lactate in the medium (instead of glucose) reduced endothelial cell proliferation rate by half when compared with glucose-containing medium (Fig. 1B). The presence of lactate together with glucose in the culture medium however did not alter endothelial cell proliferation (Fig. 1B). We then examined the influence of lactate on the endothelial expression profile of angiogenesis-related genes using dedicated TaqMan arrays on 96-well microfluidic cards. HUVEC were exposed to 10 mmol/L lactate for 6 hours to detect early changes in gene expression. We found that 7 transcripts were upregulated more than 2-fold in response to lactate and among them, IL-8/CXCL8 mRNA expression was the most responsive with an approximately 8-fold increase (vs. control HUVEC maintained in glucose-containing medium; Table 1). The increase in IL-8 gene expression was confirmed by qPCR analysis using (other) specific primers (Fig. 1C) and further validated at the protein level in a dedicated ELISA (Fig. 1D). To document a direct relationship between lactate influx and IL-8, we used a dedicated siRNA to silence the expression of the major

Table 1. Influence of lactate (10 mmol/L) on the mRNA expression profile of endothelial cells using TaqMan Gene Signature Array

Gene	Mean	SEM	Gene	Mean	SEM
SERPINC	n.d.	n.d.	SEMA3F	0.907	0.068
MMP2	0.622	0.251	TEK	0.560	0.191
ANG	1.644	0.198	TIE1	n.d.	n.d.
ANGPT1	1.032	0.216	TIMP2	1.170	0.322
ANGPT2	1.022	0.284	TIMP3	0.148	0.998
EDIL3	1.260	0.050	ANGPTL2	0.236	1.216
EPHB2	1.095	0.211	CEACAM1	1.638	0.341
FGF2	2.905	0.187	HEY1	0.409	0.804
FST	1.916	0.320	ITGAV	2.668	0.109
HGF	n.d.	n.d.	PECAM1	0.596	0.180
IL8	8.130	0.410	PGK1	1.342	0.522
MDK	1.163	0.382	XLKD1	2.619	0.050
ECGF1	1.010	0.723	KIT	n.d.	n.d.
PDGFB	1.134	0.246	NRP2	n.d.	n.d.
PROK1	n.d.	n.d.	KDR(VEGFR2)	0.637	0.457
TGFA	1.362	0.131	ENPP2	n.d.	n.d.
TGFB1	0.912	0.621	FIGF	n.d.	n.d.
TNF	n.d.	n.d.	FOXC2	1.623	0.080
VEGF	1.476	0.232	COL4A1	0.405	0.343
VEGFB	1.662	0.169	COL4A2	0.358	0.775
VEGFC	1.535	0.124	COL15A1	n.d.	n.d.
CTGF	0.700	0.144	HSPG2	0.534	0.566
FBLN5	0.588	0.377	COL18A1	0.605	0.234
THBS1	0.548	0.254	FN1	0.761	0.164
TNFSF15	3.784	0.049	COL4A3	n.d.	n.d.
ITGA4	0.364	0.799	BAI1	0.897	0.159
IL12A	1.622	0.335	CSF3	0.778	0.174
SERPINF1	n.d.	n.d.	GRN	1.888	0.238
PF4	n.d.	n.d.	THBS2	n.d.	n.d.
VASH1	n.d.	n.d.	ANGPTL4	0.598	0.602
ADAMTS1	4.442	0.628	ITGB3	1.727	0.197
AMOT	1.716	0.495	PDGFRB	n.d.	n.d.
CD44	2.070	0.405	FLT4	0.534	0.777
CDH5	0.692	0.290	NRP1	0.087	0.803
CXCL2	1.486	0.274	EDG1	0.373	0.701
SERPINB5	1.937	0.231	PROX1	0.145	0.209
VEGFR1	n.d.	n.d.	GAPDH	1.289	0.193

NOTE: Data (mean ± SEM; $n = 3$) are presented as fold-change versus control condition (glucose-containing medium).
Abbreviation: n.d. not detected.

monocarboxylate transporter MCT1 in HUVEC (unpublished data). A downregulation of more than 90% of MCT-1 expression (vs. control siRNA conditions) was confirmed at the mRNA (Fig. 1E) and protein (Fig. 1F) levels. MCT1 silencing prevented both lactate entry into endothelial cells (Fig. 1A) and lactate-induced IL-8 mRNA and protein expressions (Fig. 1C and D); MCT1 silencing reduced endothelial cell proliferation to a larger extent than lactate conditions (Fig. 1B). Of note, the ELISA test also revealed that hypoxia (1% O_2) was not able to induce IL-8 in our experimental set-up (Fig. 1D).

IL-8 induction by lactate depends on the NF-κB pathway

The known regulation of IL-8 expression by NF-κB led us to examine whether this transcription factor could mediate the lactate effects. As a first insight on the influence of lactate on NF-κB activity, we performed a TransAM assay. This experiment confirmed a significant increase in DNA binding of the p65 subunit of the NF-κB transcription complex in lactate-exposed endothelial cells (Fig. 2A). We then used a NF-κB reporter assay by transfecting HUVEC with a NF-κB–responsive luciferase plasmid (together with a GFP-encoding plasmid for normalization). We found that lactate dramatically stimulated luciferase activity (17-fold increase vs. control glucose medium, $P < 0.01$; Fig. 2B). Also, as observed for the effects of lactate on IL-8 expression (Fig. 1C and D), MCT-1 silencing blunted the increase in NF-κB reporter activity (Fig. 2B).

The recent demonstration of an autocrine IL-8–induced activation of NF-κB in endothelial cells (30) led us to verify that in our model, IL-8 was acting downstream of the lactate-induced NF-κB activity and not the converse. We therefore repeated the aforementioned experiments in the presence of an anti-IL-8–blocking antibody (10 μg/mL; Fig. 2C) or using endothelial cells wherein IL-8 expression was silenced using dedicated siRNA (Fig. 2D); a downregulation of more than 90% ($P < 0.01$, $n = 3$) of IL-8 expression (vs. control siRNA conditions) was confirmed by qPCR. We found that independently of the mode of IL-8 inhibition, lactate strongly stimulated NF-κB activity in the luciferase reporter assays (Fig. 2C and D). The use of evodiamine (500 nmol/L) as a pharmacological inhibitor of NF-κB (acting by blocking IκBα kinase activation; ref. 31) further confirmed the stimulatory effect of lactate on this transcription factor in our experimental model (Fig. 2C).

Lactate stimulates the NF-κB/IL-8 pathway in a ROS- and IκBα-dependent manner

To further dissect the pathway linking lactate stimulation and NF-κB/IL-8 induction, we examined the role of ROS usually described as key triggers of NF-κB activity. We first treated endothelial cells with the ROS scavenger *N*-acetylcysteine (NAC) and found that in these conditions, both lactate-induced NF-κB activity (Fig. 3A) and IL-8 expression (Fig. 3B) were completely abrogated, as determined using the luciferase reporter assay and qPCR, respectively. The use of the ROS fluorescent dye 2′-7′-dichlorofluorescin diacetate confirmed that the exposure of endothelial cells to 10 mmol/L lactate led to a rapid increase in ROS production (vs. control glucose conditions; Fig. 3C). Importantly, a similar increase in ROS production was observed when cells were exposed to both glucose and lactate (Fig. 3C). Because ROS-mediated activation of NF-κB is classically proposed to be dependent on IκBα phosphorylation/degradation (which favors the release of active NF-κB subunits; 32), we then examined the effect of lactate on IκBα serines 32 and 36 phosphorylations. We found that lactate supplementation (alone or together with glucose)

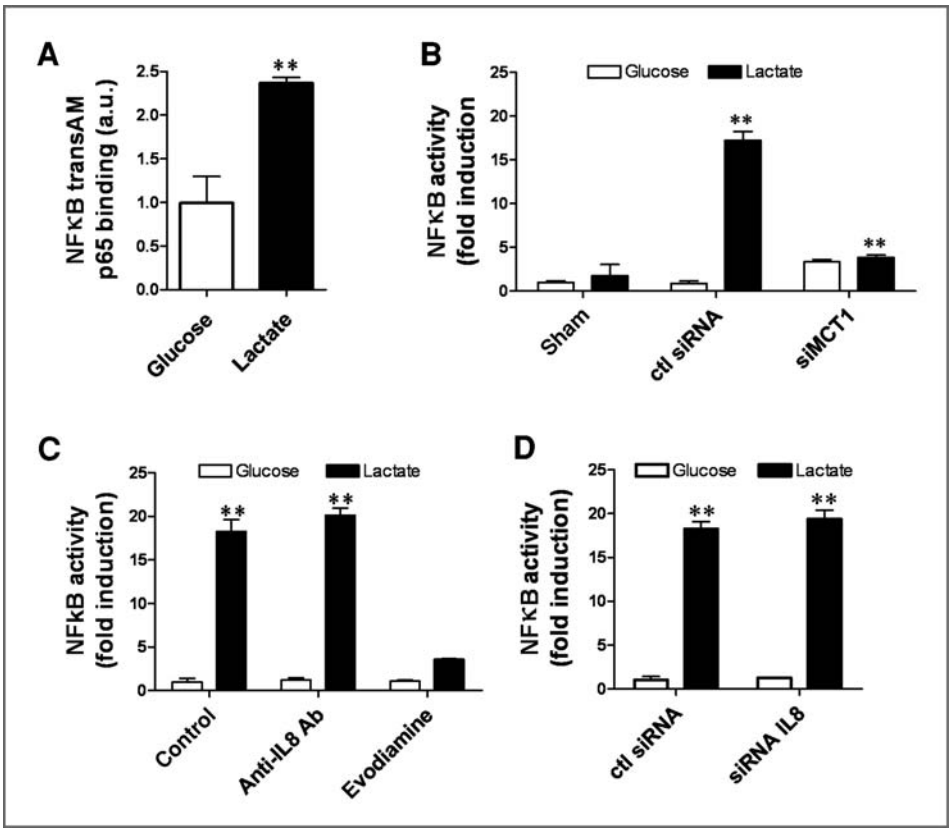

Figure 2. Lactate stimulates NF-κB activity in endothelial cells in a MCT1-dependent manner. A, bar graph represents the extent of p65 subunit detected in a NF-κB TransAM assay from nuclear extracts of endothelial cells exposed for 6 hours to glucose- or lactate (10 mmol/L)-containing medium ($P < 0.01$, $n = 3$). Other bar graphs represent the NF-κB activity (normalized per cell numbers) determined using a dedicated luciferase reporter assay (see Materials and Methods) from endothelial cells cultured for 6 hours in glucose- (open bars) or lactate- (black bars) containing medium (B) after transfection with a MCT1-targeting siRNA (vs. sham conditions and control siRNA), (C) after treatment with 10 μg/mL anti-IL-8–blocking antibody or 500 nmol/L evodiamine, (D) after transfection with a IL-8–targeting siRNA (vs. control siRNA); each bar represents the mean ± SEM of 3 independent experiments (**, $P < 0.01$).

led to a net increase in IκBα phosphorylation, a process that we also found to be associated with IκBα degradation, as documented by immunoblotting (Fig. 3D).

2-oxoglutarate inhibits while PHD2-silencing mimics the effects of lactate on the NF-κB/IL-8 signaling pathway

A prolyl hydroxylase (PHD)-dependent activation of NF-κB activity was previously reported to occur through the IκBα pathway (33–35). Considering that PHD activity requires 2-oxoglutarate as cosubstrate and may thereby be influenced by other carboxylate metabolic intermediates (see Introduction), we examined whether in endothelial cells, lactate competition with 2-oxoglutarate could account for the observed increase in NF-κB/IL-8 expression. We found that 2-oxoglutarate dose-dependently prevented lactate-induced NF-κB activity (Fig. 4A), as determined in a luciferase reporter assay. We also found that PHD2-silencing in endothelial cells led to a net increase in both NF-κB activity (Fig. 4B) and IL-8 expression (Fig. 4C) under basal conditions (i.e., in lactate-free glucose-containing medium) and failed to further stimulate the NF-κB/IL-8 expression pathway in response to lactate (Fig. 4B and C). Downregulation of more than 90% of PHD-2 expression (vs. control siRNA conditions) was confirmed by qPCR (Fig. 4D). We also documented that lactate-induced IL-8 expression was strongly inhibited by 2-oxoglutarate and diphenylene iodonium chloride (DPI), a potent inhibitor of NADPH oxidase (a major enzymatic source of ROS in endothelial cells; Fig. 4C). Interestingly, PHD2-silencing failed to stimulate IL-8 expression in glucose-containing medium when DPI was present (Fig. 4C), suggesting that both PHD2 inhibition and ROS production are required to promote the NF-κB pathway in endothelial cells.

MCT4-driven release of lactate from cancer cells stimulates IL-8 production together with tumor angiogenesis and perfusion

To examine the NF-κB/IL-8–driven effects of lactate *in vivo*, we used tumor cells genetically modified for their capacity to handle lactate. Accordingly, we established clones from the WiDr human colorectal cancer cell line selected for stable expression of shRNA directed against MCT1 or MCT4. We found that WiDr cells express both types of MCT transporters and that the use of dedicated shRNA led to the silencing of MCT1 expression (91.2 ± 6% downregulation; Fig. 5A) and MCT4 (96.5 ± 9% downregulation) (Fig. 5B), respectively. We found that although MCT1-silencing did not prevent the efflux of lactate induced under hypoxia (Fig. 5A, bottom), MCT4-silencing had a dramatic effect on the capacity of WiDr cells to release lactate in the same hypoxic conditions (Fig. 5B, bottom). Measurements of cell proliferation rate *in vitro* however did not reveal any difference between shMCT1 and shMCT4 WiDr cell clones (Fig. 5C). Of note, the extents of lactate release in shMCT1 WiDr cells and sham-transfected WiDr were not significantly different, in agreement with a major role of this transporter in the influx-–and not the efflux-–of lactate in this cell type (6).

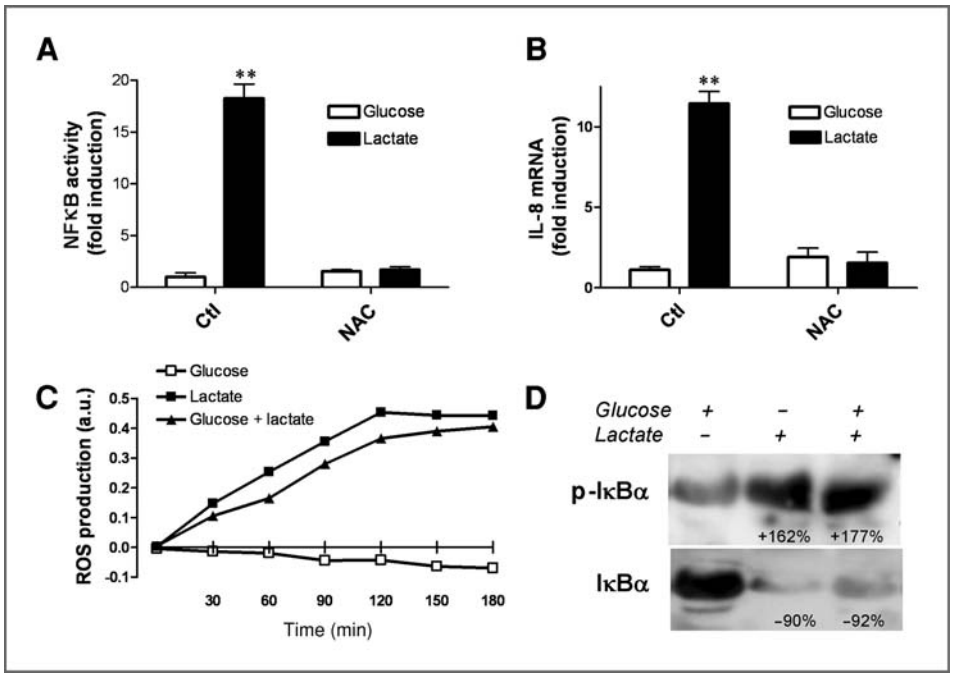

Figure 3. Lactate induces the NF-κB/IL-8 pathway in endothelial cells in a ROS- and IKK-dependent manner. Bar graphs represent (A) NF-κB activity determined using a dedicated luciferase reporter assay and (B) IL-8 mRNA expression determined by qPCR from endothelial cells cultured in the presence (or not) of 10 mmol/L NAC for 6 hours in glucose- (open bars) or lactate- (black bars) containing medium. Each bar represents the mean ± SEM of 3 to 4 independent experiments (**, $P < 0.01$). C, graph represents the production of ROS (arbitrary units, a.u.), as determined using the cell permeant fluorescent indicator DCF-DA (25 μmol/L), from endothelial cells exposed for the indicated periods of time to fresh medium containing glucose, lactate, or both; $n = 3$, SEM are smaller than symbols. D, representative phospho-IκBα (serine 32 and 36) and total IκBα immunoblotting from endothelial cells exposed for 15 minutes to glucose, lactate, or both; mean changes in signal intensity resulting from 3 independent experiments are indicated.

To validate the functional consequences of a deficit in lactate release, we first used the conditioned medium (CM) collected from either shMCT1 or shMCT4 WiDr cells to treat endothelial cells. We found that IL-8 expression (as determined by qPCR) was stimulated by CM collected from hypoxic shMCT1 cells but not altered by the exposure to CM from hypoxic shMCT4 cells (Fig. 5D). In another set of experiments, we injected s.c. plugs of Matrigel containing 5×10^4 HUVEC together with either 5×10^5 WiDr shMCT1 cells or 5×10^5 WiDr shMCT4 cells. We found that tumor growth from the plug containing shMCT4 WiDr cells was reduced (vs. shMCT1 cells containing plug; Fig. 5E). We also verified that tumor lactate (Fig. 5F) and IL-8 (Fig. 5G) contents were reduced in shMCT4-expressing tumors (vs. shMCT1 tumors). Importantly, this was associated with a dramatic inhibition of angiogenesis as determined by CD31 immunostaining of vascular structures, together with a reduction in tumor blood flow as measured by laser Doppler imaging (Fig. 5H, see bottom for quantification). We repeated these experiments using a MDA-MB231 breast cancer cell clone wherein MCT4 was also silenced and found a similar phenotype (i.e., reduced CD31-labeled microvascular density and tumor perfusion; see Fig. 5I). For both tumors, the use of a CD31 antibody selective for mouse tissues (36) did, however, not lead to any specific staining, indicating that the vascular signal was of human origin and thus corresponded to HUVEC.

Lactate-dependent induction of IL-8 expression supports angiogenesis and tumor growth

To dissect the NF-κB/IL-8–driven proangiogenic effects of lactate, we first measured the migration of HUVEC in a modified Boyden chamber. Migration was determined after 24 hours by counting DAPI-stained cells on the bottom face of the filter. To first validate the IL-8 capacity to drive cell migration in this assay, recombinant IL-8 protein was added to glucose-containing medium in the upper part of the well. A 10-fold increase in the number of migrated endothelial cells was observed (vs. untreated conditions; Fig. 6A). Replacement of glucose by lactate (10 mmol/L) in the medium of the upper chamber led to a similar stimulation of endothelial cell migration. This promigratory effect of lactate was IL-8—dependent, as migration was completely blocked by either a dedicated IL-8 siRNA cell pretreatment or the presence of a blocking anti-IL-8 antibody in the upper well compartment (Fig. 6A). The use of NAC and evodiamine similarly reduced the capacity of lactate to promote the motility of endothelial cells (Fig. 6A)

We next examined how interfering with lactate cellular uptake and consecutive increase in IL-8 expression could influence the capacity of endothelial cells to form tubes when plated on Matrigel. We first showed that lactate exposure stimulates the formation of an endothelial network in these experimental conditions (Fig. 6B). We then documented that siRNA directed against either MCT-1 or IL-8 prevented

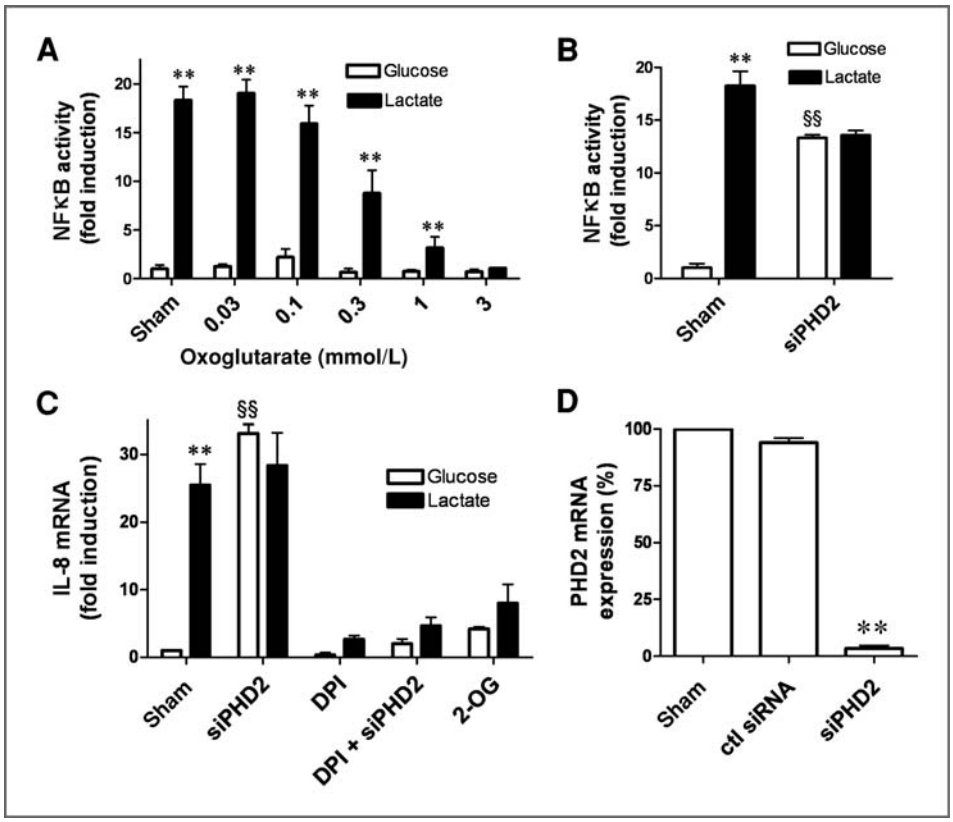

Figure 4. Lactate induces the NF-κB/IL-8 pathway in endothelial cells in a 2-oxoglutarate/PHD2-dependent manner. Bar graphs represent NF-κB activity determined using a dedicated luciferase reporter assay in the presence of (A) increasing concentrations of 2-oxoglutarate (2-OG) and (B) after PHD2-targeting siRNA transfection in glucose (open bars) or lactate (black bars; **, $P < 0.01$ vs. corresponding glucose condition, §§, $P < 0.01$ vs. corresponding *sham* glucose condition, $n = 3$). C, bar graph represents IL-8 mRNA expression determined by qPCR from endothelial cells treated as before (PHD2 siRNA or 1 mmol/L 2-OG), in the presence (or not) of flavoenzyme inhibitor diphenyleneiodonium chloride (DPI; 10 μmol/L) for 6 hours in glucose- (open bars) or lactate- (black bars) containing medium (**, $P < 0.01$, §§, $P < 0.01$ as before, $n = 3$). D, PHD2-silencing with dedicated siRNA (vs. sham conditions and control siRNA) was confirmed (24 hours posttransfection) by qPCR ($P < 0.01$, $n = 3$).

lactate-driven formation of tubes (Fig. 6B and C, respectively, for quantification). Importantly, the addition of recombinant IL-8 to IL-8–siRNA–treated endothelial cells rescued tubulogenesis (Fig. 6B and C). As observed in Figure. 6A, the use of NAC and evodiamine confirmed a role for ROS/NF-κB in the lactate-dependent IL-8–driven formation of endothelial tubes (Fig. 6C). Also, in adequation with results of Figure 4A and B, 2-oxoglutarate blunted the tubulogenic response to lactate and PHD2 silencing in glucose-containing medium recapitulated the effects of lactate with a strong stimulation of tube formation (Fig. 6C).

Finally, to further validate the *in vivo* relevance of the lactate/IL-8 proangiogenic pathway, we injected s.c. 2 plugs of Matrigel containing 5×10^5 wild-type WiDr cells and 5×10^4 HUVEC supplemented with of without 100 μg/mL IL-8–blocking antibody. In this tumor model of lactate-driven angiogenesis, we found that the presence of anti-IL-8–blocking antibodies within the Matrigel plug delayed tumor growth (Fig. 6D) and considerably reduced the development of the tumor vasculature, as revealed by anti-CD31 immunostaining (Fig. 6E, top; $-75 \pm 13\%$ vs. control, $P < 0.01$, $n = 5$). Finally, to prove the role of MCT1 *in vivo*, we similarly coinjected WiDr cells and HUVEC pretreated with MCT1 siRNA. We found that tumor growth and development of the microvascular network ($-66 \pm 21\%$ vs. control, $P < 0.05$, $n = 5$) were both inhibited in response to MCT1 silencing in endothelial cells (Fig. 6D and E, bottom).

Discussion

Major findings of this study are the identification of a lactate/NF-κB signaling pathway in endothelial cells, the existence of a lactate-driven, feed-forward IL-8 autocrine loop driving angiogenesis in tumors and the key roles of monocarboxylate transporters MCT1 and MCT4 in this lactate-based dialog between cancer cells and endothelial cells. Our data indeed support a model according to which lactate released from tumor cells through MCT4 may be taken up by endothelial cells via the MCT1 transporter and consecutively stimulate angiogenesis through NF-κB/IL-8 signaling (Supplementary Fig. S1); all these lactate-driven signaling events may importantly occur in the presence of glucose.

We identified key players acting upstream and downstream of this pathway in endothelial cells. We found that ROS were

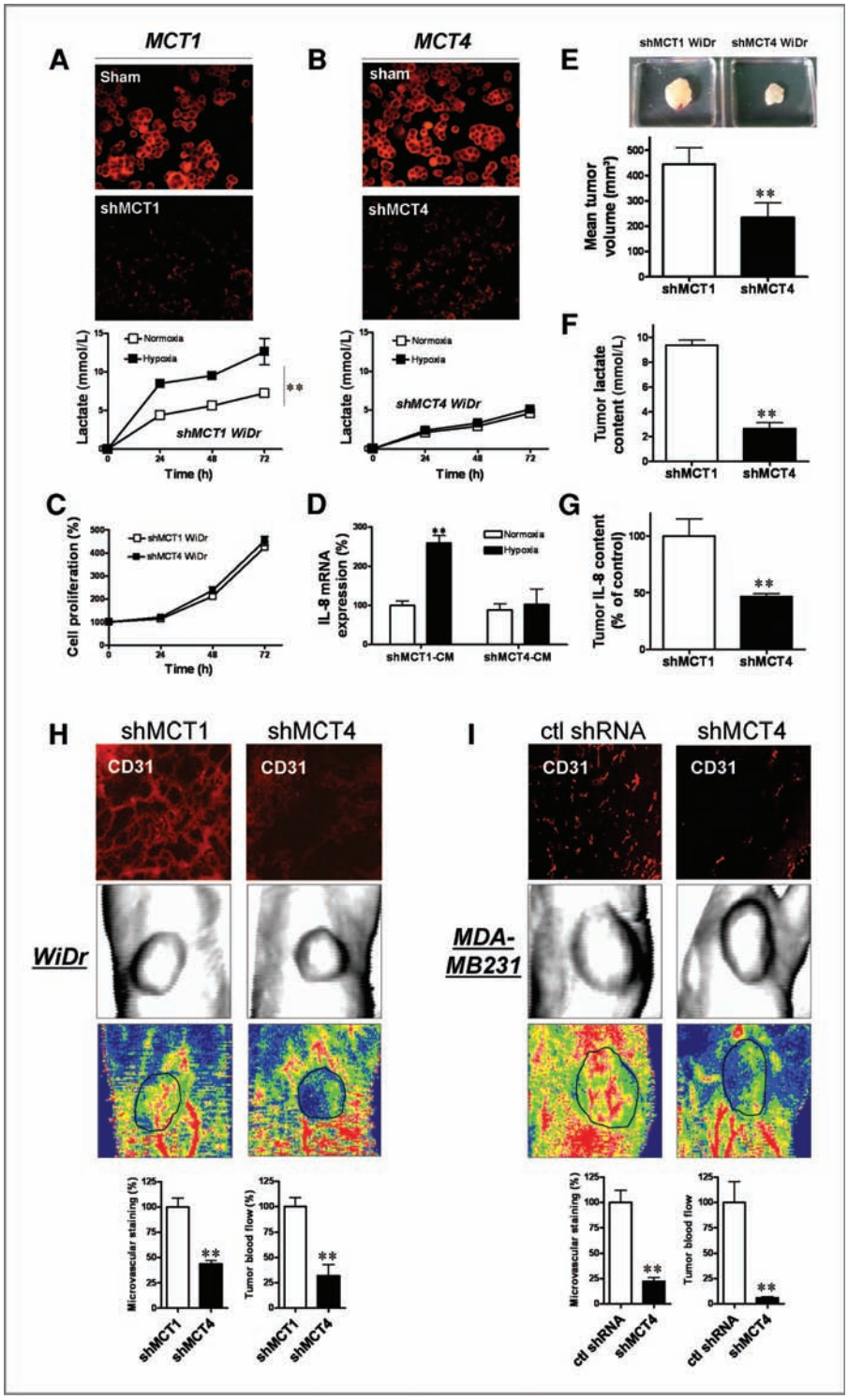

Figure 5. Lactate efflux through tumor cell MCT4 stimulates IL-8 expression in endothelial cells and promotes tumor vascular development *in vivo*. WiDr colorectal cancer cells were sham or stably transfected with a MCT1- or MCT4-targeting shRNA. Representative photographs of (A) MCT1 and (B) MCT4 immunostaining. Graphs represent the time course of lactate release from shMCT1 WiDr cells (A, bottom) and shMCT4 WiDr cells (B, bottom) cultured under normoxic (open symbols) or 1% O_2-hypoxia (black symbols; *, $P < 0.01$, $n = 4$). C, graph represents the *in vitro* proliferation rate of shMCT1- or shMCT4 WiDr cells ($n = 3$). D, bar graph represents IL-8 mRNA expression determined by qPCR from endothelial cells cultured for 6 hours in the presence of CM of shMCT1- or shMCT4 WiDr cells maintained (for 72 hours) under normoxia (open bars) or hypoxia (black bars; *, $P < 0.01$, $n = 3$). E, representative photographs of tumors removed from mice injected (14 days before) with Matrigel plug containing 5×10^4 endothelial cells mixed either with 5×10^5 shMCT1 WiDr cells or 5×10^5 shMCT4 WiDr cells. Bar graph (E, bottom) represents the mean tumor volume of corresponding tumors ($n = 5$; $P < 0.01$). Bar graphs represent the intratumor lactate (F) and IL-8 (G) concentrations in the tumors described in E. Representative photographs of CD31 immunostaining, laser Doppler imaging (including reconstituted tumor photograph) of WiDr (H) and MDA-MB231 (I) tumors. Quantifications of corresponding microvascular density and perfusion are presented in bar graphs (H and I, bottom).

produced in endothelial cells in response to lactate and that ROS inhibitors prevented lactate-induced activation of NF-κB and IL-8 expression. Also, we showed that the PHD cosubstrate 2-oxoglutatrate could prevent the effects of lactate on NF-κB activation and that conversely, PHD2 silencing recapitulated them in normal glucose conditions. We further documented the stimulatory effects of lactate on IκBα phosphorylation and consecutive degradation in endothelial cells, a process known to promote translocation of freed NF-κB activation into the nucleus for transcriptional regulation (32). Using siRNA directed against IL-8 (rescued or not with recombinant IL-8), we showed that this autocrine pathway

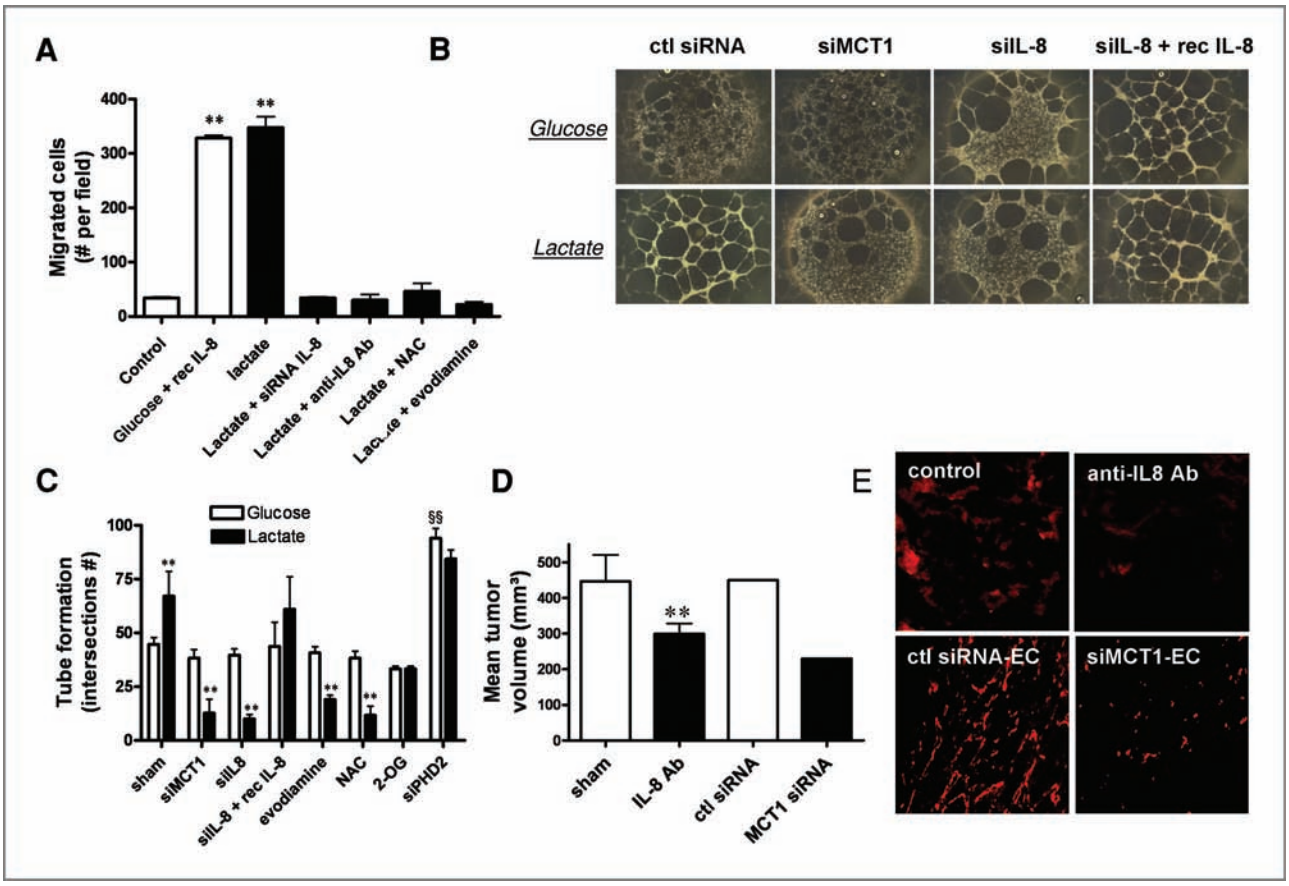

Figure 6. Lactate stimulates IL-8–dependent angiogenesis *in vitro* and *in vivo* in a MCT1-dependent manner. A, bar graph shows the extent of (24 hours) migrated endothelial cells (per microscopic field) through Matrigel coated-filters in response to 5 ng/mL recombinant IL-8 (in glucose medium) or in response to lactate (added to the upper well compartment), including after cell transfection with a dedicated IL-8-targeting siRNA or concomitant incubation with a blocking anti-IL-8 antibody, 10 mmol/L NAC or 500 nmol/L evodiamine (**, $P < 0.01$, $n = 4$). B, representative photographs of (24 hours) tube formation in glucose- or lactate-containing medium from Matrigel-plated endothelial cells after transfection with a control siRNA, a MCT1-targeting siRNA, or an IL-8–targeting siRNA with or without addition of recombinant IL-8. C, bar graph represents the quantification of tubulogeneis experiments as described in B as well as in similar assays performed in the presence of evodiamine, NAC, or 2-oxoglutarate and after transfection with PHD2-targeting siRNA (**, $P < 0.01$ vs. corresponding glucose conditions; §§, $P < 0.01$ vs. sham condition, $n = 4$). D, bar graph represents the mean volumes of tumors removed from mice injected (14 days before) with Matrigel plug containing 5×10^5 wild-type WiDr cells mixed with 5×10^4 endothelial cells in the presence (or the absence) of an anti-IL-8–blocking antibody or following pretreatment of HUVEC with a MCT1-targeting siRNA ($n = 5$–6 mice per group; **, $P < 0.01$). E, representative photographs of CD31 immunostaining of corresponding tumor sections.

accounts for most of the proangiogenic effects of lactate in endothelial cells. Importantly, we validated *in vivo* that the release of lactate by cancer cells can effectively contribute to the development of the tumor vasculature by stimulating the IL-8 pathway. A blocking antibody directed against IL-8 could indeed prevent the stimulation of angiogenesis (Fig. 6E) and reduce tumor growth (Fig. 6D) in a model where lactate efflux through the MCT4 transporter is a key trigger of the development of tumor vasculature (Fig. 5H and I).

Lactate was previously documented to stimulate angiogenesis (14–16) through activation of the VEGF/VEGFR2 signaling pathway (16–20). Although it may be difficult to discriminate between the role of hypoxia and lactate in triggering VEGF signaling *in vivo*, our finding of NF-κB acting as a lactate-responsive transcription factor unravels a pathway which may link tumor cell metabolism and angiogenesis independently of the O_2 conditions. An interesting parallel may be drawn with previous studies by Verma and colleagues who reported that pyruvate, lactate, and several TCA cycle intermediates can stabilize HIF-1 through inhibition of PHD enzymes (23, 24). These data are proposed to support the Warburg effect, that is, the capacity of nonhypoxic tumor cells to exploit glycolysis without a need for coupling to oxidative phosphorylations to support the high biosynthetic and energy demands of proliferating cells. Our study allows to extend this paradigm to tumor angiogenesis and supports a central role of lactate bridging avid glucose metabolism and key aspects of malignancy, namely tumor cell proliferation and angiogenesis (Supplementary Fig. S1).

Interestingly, reduction in PHD activity appears to be the common denominator in the stabilization of HIF and NF-κB observed in response to lactate. In particular, our data are in

line with the work of Cummins and colleagues (34) who previously showed that hypoxia may activate NF-κB through a decreased PHD1-dependent hydroxylation of IKKβ and consecutive phosphorylation-dependent degradation of IκBα. In a more recent study, Chan and colleagues, starting from the observation of a frequent loss of PHD2 expression in cancers, documented that the tumor suppressor gene potential of this hydroxylase was associated with an increased NF-κB activation in tumor cells (33). To reproduce the loss of PHD2 expression, these authors used PHD2-silenced cancer cells and documented that mouse injection with these modified tumor cells led to the development of more vascularized tumors. The effects of lactate observed in our study therefore mimic the effects of a downmodulation of PHD2, leading *in fine* to the activation of NF-κB–driven angiogenic cascades. Interestingly, we found that lactate-driven angiogenesis leads *in vivo* to a net increase in tumor perfusion indicating that the stimulated NF-κB/IL-8 pathway also contributes to the maturation of the tumor neovasculature. These data may be related to a recent study by Mazzone and colleagues who documented that heterozygous deficiency of PHD2 normalized the tumor endothelial lining, resulting in improved tumor perfusion (37). The same authors further documented that haplodeficiency of PHD2 restores tumor oxygenation and thus possibly induce a metabolic shift to a more oxidative, less malignant phenotype. Similarly, our data support the hypothesis that in response to lactate exposure, endothelial cells may exhibit alterations in their metabolic phenotype leading to increased cell survival in glucose-free conditions (Fig. 1B). The ROS production observed in endothelial cells in response to lactate could actually arise from the activation of the NAD(P)H oxidase by NADH accumulation resulting from the conversion of lactate into pyruvate, as we previously reported in tumor cells (6).

In conclusion, our study provides a new rationale for associating elevated lactate concentrations in tumors and negative outcomes for patients. These results further support the current enthusiasm for new cancer treatments targeting metabolic pathways (38). In particular, inhibitors of MCT1 and/or MCT4 bear the promise of interfering with the subtle exchanges of lactate between tumor cells and endothelial cells, and to indirectly attenuate the IL-8 effect on tumor vascular development and associated tumor burden.

Disclosure of Potential Conflicts of Interest

No potential conflicts of interest were disclosed.

Grant Support

This work was supported by grants from the Fonds de la Recherche Scientifique FRS-FNRS, the Fonds de la Recherche Scientifique Médicale, the Télévie, the Belgian Federation against cancer, the J. Maisin Foundation, the Région Bruxelles-Capitale, an Action de Recherche Concertée (ARC 09/14-020), and the European Research Council FP7/2007-2013 (grant #243188 to P. Sonveaux). O. Feron is a FRS-FNRS Research Director and P. Sonveaux is a FRS-FNRS Research Associate.

The costs of publication of this article were defrayed in part by the payment of page charges. This article must therefore be hereby marked *advertisement* in accordance with 18 U.S.C. Section 1734 solely to indicate this fact.

Received August 1, 2010; revised December 15, 2010; accepted January 25, 2011; published OnlineFirst February 7, 2011.

References

1. Feron O. Pyruvate into lactate and back: from the Warburg effect to symbiotic energy fuel exchange in cancer cells. Radiother Oncol 2009;92:329–33.
2. DeBerardinis RJ, Lum JJ, Hatzivassiliou G, Thompson CB. The biology of cancer: metabolic reprogramming fuels cell growth and proliferation. Cell Metab 2008;7:11–20.
3. DeBerardinis RJ, Mancuso A, Daikhin E, Nissim I, Yudkoff M, Wehrli S, et al. Beyond aerobic glycolysis: transformed cells can engage in glutamine metabolism that exceeds the requirement for protein and nucleotide synthesis. Proc Natl Acad Sci U S A 2007;104:19345–50.
4. Gladden LB. Lactate metabolism: a new paradigm for the third millennium. J Physiol 2004;558:5–30.
5. Philp A, Macdonald AL, Watt PW. Lactate–a signal coordinating cell and systemic function. J Exp Biol 2005;208:4561–75.
6. Sonveaux P, Vegran F, Schroeder T, Wergin MC, Verrax J, Rabbani ZN, et al. Targeting lactate-fueled respiration selectively kills hypoxic tumor cells in mice. J Clin Invest 2008;118:3930–42.
7. Walenta S, Schroeder T, Mueller-Klieser W. Lactate in solid malignant tumors: potential basis of a metabolic classification in clinical oncology. Curr Med Chem 2004;11:2195–204.
8. Walenta S, Mueller-Klieser WF. Lactate: mirror and motor of tumor malignancy. Semin Radiat Oncol 2004;14:267–74.
9. Quennet V, Yaromina A, Zips D, Rosner A, Walenta S, Baumann M, et al. Tumor lactate content predicts for response to fractionated irradiation of human squamous cell carcinomas in nude mice. Radiother Oncol 2006;81:130–5.
10. Brizel DM, Schroeder T, Scher RL, Walenta S, Clough RW, Dewhirst MW, et al. Elevated tumor lactate concentrations predict for an increased risk of metastases in head-and-neck cancer. Int J Radiat Oncol Biol Phys 2001;51:349–53.
11. Walenta S, Wetterling M, Lehrke M, Schwickert G, Sundfor K, Rofstad EK, et al. High lactate levels predict likelihood of metastases, tumor recurrence, and restricted patient survival in human cervical cancers. Cancer Res 2000;60:916–21.
12. Walenta S, Salameh A, Lyng H, Evensen JF, Mitze M, Rofstad EK, et al. Correlation of high lactate levels in head and neck tumors with incidence of metastasis. Am J Pathol 1997;150:409–15.
13. Schwickert G, Walenta S, Sundfor K, Rofstad EK, Mueller-Klieser W. Correlation of high lactate levels in human cervical cancer with incidence of metastasis. Cancer Res 1995;55:4757–9.
14. Crowther M, Brown NJ, Bishop ET, Lewis CE. Microenvironmental influence on macrophage regulation of angiogenesis in wounds and malignant tumors. J Leukoc Biol 2001;70:478–90.
15. Ghani QP, Wagner S, Hussain MZ. Role of ADP-ribosylation in wound repair. The contributions of Thomas K. Hunt, MD. Wound Repair Regen 2003;11:439–44.
16. Hunt TK, Aslam RS, Beckert S, Wagner S, Ghani QP, Hussain MZ, et al. Aerobically derived lactate stimulates revascularization and tissue repair via redox mechanisms. Antioxid Redox Signal 2007;9:1115–24.
17. Beckert S, Farrahi F, Aslam RS, Scheuenstuhl H, Konigsrainer A, Hussain MZ, et al. Lactate stimulates endothelial cell migration. Wound Repair Regen 2006;14:321–4.
18. Kumar VB, Viji RI, Kiran MS, Sudhakaran PR. Endothelial cell response to lactate: implication of PAR modification of VEGF. J Cell Physiol 2007;211:477–85.

19. Burns PA, Wilson DJ. Angiogenesis mediated by metabolites is dependent on vascular endothelial growth factor (VEGF). Angiogenesis 2003;6:73–7.
20. Xiong M, Elson G, Legarda D, Leibovich SJ. Production of vascular endothelial growth factor by murine macrophages: regulation by hypoxia, lactate, and the inducible nitric oxide synthase pathway. Am J Pathol 1998;153:587–98.
21. Schmid SA, Gaumann A, Wondrak M, Eckermann C, Schulte S, Mueller-Klieser W, et al. Lactate adversely affects the in vitro formation of endothelial cell tubular structures through the action of TGF-beta1. Exp Cell Res 2007;313:2531–49.
22. Semenza GL. Targeting HIF-1 for cancer therapy. Nat Rev Cancer 2003;3:721–32.
23. Lu H, Dalgard CL, Mohyeldin A, Mcfate T, Tait AS, Verma A. Reversible inactivation of HIF-1 prolyl hydroxylases allows cell metabolism to control basal HIF-1. J Biol Chem 2005;280:41928–39.
24. Lu H, Forbes RA, Verma A. Hypoxia-inducible factor 1 activation by aerobic glycolysis implicates the Warburg effect in carcinogenesis. J Biol Chem 2002;277:23111–5.
25. Semenza GL. Regulation of cancer cell metabolism by hypoxia-inducible factor 1. Semin Cancer Biol 2009;19:12–6.
26. Sonveaux P, Martinive P, DeWever J, Batova Z, Daneau G, Pelat M, et al. Caveolin-1 expression is critical for vascular endothelial growth factor-induced ischemic hindlimb collateralization and nitric oxide-mediated angiogenesis. Circ Res 2004;95:154–61.
27. Daneau G, Boidot R, Martinive P, Feron O. Identification of cyclooxygenase-2 as a major actor of the transcriptomic adaptation of endothelial and tumor cells to cyclic hypoxia: effect on angiogenesis and metastases. Clin Cancer Res 2010;16:410–9.
28. Martinive P, Defresne F, Bouzin C, Saliez J, Lair F, Gregoire V, et al. Preconditioning of the tumor vasculature and tumor cells by intermittent hypoxia: implications for anticancer therapies. Cancer Res 2006;66:11736–44.
29. DeWever J, Frerart F, Bouzin C, Baudelet C, Ansiaux R, Sonveaux P, et al. Caveolin-1 is critical for the maturation of tumor blood vessels through the regulation of both endothelial tube formation and mural cell recruitment. Am J Pathol 2007;171:1619–28.
30. Martin D, Galisteo R, Gutkind JS. CXCL8/IL8 stimulates vascular endothelial growth factor (VEGF) expression and the autocrine activation of VEGFR2 in endothelial cells by activating *NFkappaB* through the CBM (Carma3/Bcl10/Malt1) complex. J Biol Chem 2009;284:6038–42.
31. Takada Y, Kobayashi Y, Aggarwal BB. Evodiamine abolishes constitutive and inducible *NF-kappaB* activation by inhibiting IkappaBalpha kinase activation, thereby suppressing *NF-kappaB*-regulated antiapoptotic and metastatic gene expression, up-regulating apoptosis, and inhibiting invasion. J Biol Chem 2005;280:17203–12.
32. Gloire G, Legrand-Poels S, Piette J. *NF-kappaB* activation by reactive oxygen species: fifteen years later. Biochem Pharmacol 2006;72:1493–505.
33. Chan DA, Kawahara TL, Sutphin PD, Chang HY, Chi JT, Giaccia AJ. Tumor vasculature is regulated by PHD2-mediated angiogenesis and bone marrow-derived cell recruitment. Cancer Cell 2009;15:527–38.
34. Cummins EP, Berra E, Comerford KM, Ginouves A, Fitzgerald KT, Seeballuck F, et al. Prolyl hydroxylase-1 negatively regulates IkappaB kinase-beta, giving insight into hypoxia-induced NFkappaB activity. Proc Natl Acad Sci U S A 2006;103:18154–9.
35. Fu J, Taubman MB. Prolyl hydroxylase EGLN3 regulates skeletal myoblast differentiation through an NF-kappaB-dependent pathway. J Biol Chem 2010;285:8927–35.
36. Van Eyck AS, Bouzin C, Feron O, Romeu L, Van LA, Donnez J, et al. Both host and graft vessels contribute to revascularization of xenografted human ovarian tissue in a murine model. Fertil Steril 2010;93:1676–85.
37. Mazzone M, Dettori D, Leite de OR, Loges S, Schmidt T, Jonckx B, et al. Heterozygous deficiency of PHD2 restores tumor oxygenation and inhibits metastasis via endothelial normalization. Cell 2009;136:839–51.
38. Tennant DA, Duran RV, Gottlieb E. Targeting metabolic transformation for cancer therapy. Nat Rev Cancer 2010;10:267–77.